

ChemComm

Accepted Manuscript



This is an *Accepted Manuscript*, which has been through the Royal Society of Chemistry peer review process and has been accepted for publication.

Accepted Manuscripts are published online shortly after acceptance, before technical editing, formatting and proof reading. Using this free service, authors can make their results available to the community, in citable form, before we publish the edited article. We will replace this *Accepted Manuscript* with the edited and formatted *Advance Article* as soon as it is available.

You can find more information about *Accepted Manuscripts* in the [Information for Authors](#).

Please note that technical editing may introduce minor changes to the text and/or graphics, which may alter content. The journal's standard [Terms & Conditions](#) and the [Ethical guidelines](#) still apply. In no event shall the Royal Society of Chemistry be held responsible for any errors or omissions in this *Accepted Manuscript* or any consequences arising from the use of any information it contains.

COMMUNICATION

Reduced TiO₂ rutile nanorods with well-defined facet and their visible-light photocatalytic activity

Cite this: DOI: 10.1039/x0xx00000x

Zhao Zhao,^{ab} Huaqiao Tan,^{a*} Haifeng Zhao, Yang Lv,^c Li-Jing Zhou,^d Yujiang Song,^c and Zaicheng Sun^{a*}

Received 00th January 2012,

Accepted 00th January 2012

DOI: 10.1039/x0xx00000x

www.rsc.org/

Abstract. Stable reduced TiO₂ rutile nanorods with well-defined facets was prepared by solvothermal route in the presence of Zn powder. The oxygen vacancy in the TiO₂ nanorods, which can be tuned by the amount of Zn, results in a narrow band gap and visible-light photocatalytic activity.

Titanium dioxide (TiO₂) has been extensively employed in many solar energy conversion applications such as photovoltaic, photocatalytic organic waste degradation, and water splitting for H₂ production and become a promising photocatalyst due to its good chemical, thermal and biological stability.¹ However, the large band gap of TiO₂ severely hinders its practical application because TiO₂ only absorbs UV light, which is lower than 5% of full solar spectrum. Many efforts have been proposed to make TiO₂ with visible-light response. For example, doped TiO₂ with metal or non-metal ions exhibited a broad visible light absorption and great performance.² Recently, reduced TiO₂ (TiO_{2-x}), incorporating Ti³⁺ and/or oxygen vacancies in TiO₂, has emerged as an effective route to obtain visible-light photoactivity.³ However, theoretical work has suggested that, in order to achieve an efficient activity in the visible spectrum, the concentration of Ti³⁺ must be sufficiently high to induce a continuous vacancy band of electronic states just below the conduction band edge of TiO₂.⁴ Otherwise, a low Ti³⁺ doping concentration only creates localized oxygen vacancy states that deteriorate the electron mobility and exhibit a negligible visible photo activity. This is due to the fact that the energy of the scattered doping states is largely (0.75–1.18 eV) below the conduction band edge of TiO₂ and the occupying photo-electrons are not adequately reactive and/or mobile for desired electrochemical reactions.⁵⁻⁷ Therefore, doping with a high concentration of Ti³⁺ in TiO₂ is essential to enhance the photocatalytic activity in the visible region.

Several techniques have been reported to produce TiO_{2-x} including thermal treatment under vacuum⁸ or reducing conditions,^{3b, 9-11} electrons¹² or Ar⁺ ions¹³ bombardment, and hydrothermal treatment.^{3d, 3f, 14} Most reports start from TiO₂, from which a fraction of the Ti⁴⁺ ions is reduced to Ti³⁺ under harsh reducing conditions such as high temperature in reducing gas (H₂ or CO). Furthermore, since the reduction occurs mainly on the surface of TiO₂, the oxygen vacancies are usually not enough stable, even in air. The TiO_{2-x} with

surface oxygen vacancy (Ti³⁺) could be easily oxidized to TiO₂ within a short period. Thus it is still a great challenge to develop a facile synthetic route to prepare stable reduced TiO₂ nanocrystals with well-defined facets.

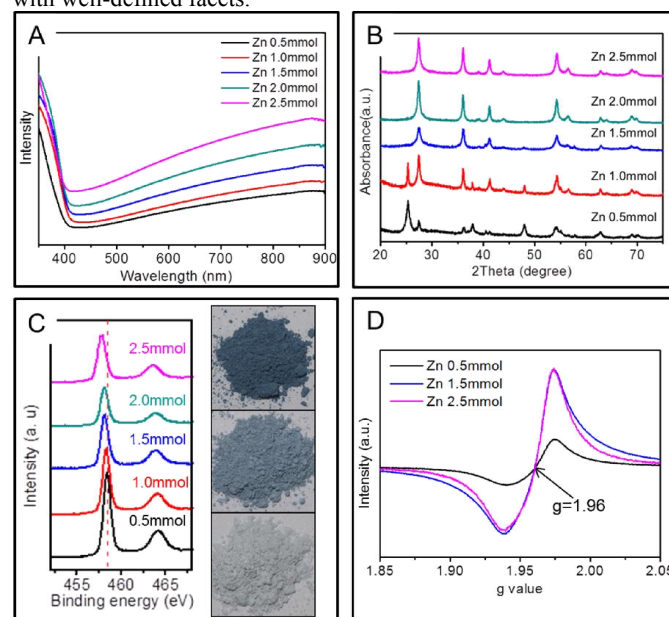


Fig.1 The characterizations of reduced TiO₂ prepared by solvothermal reaction with different amount Zn powder (line color black, red, blue, cyan, and purple for 0.5, 1.0, 1.5, 2.0, and 2.5 mmol, respectively). (A) UV-visible absorbance spectra (converted from diffuse reflectance spectra), (B) XRD patterns, (C) High resolution Ti 2p XPS spectra, insets are optical images of reduced TiO₂ obtained from 2.5, 1.5 and 0.5 mmol of Zn powder from top to bottom. (D) EPR spectra.

In this report, we developed a simple and facile solvothermal strategy of preparing highly active and stable TiO_{2-x} rutile nanorods exposed (110) facets and tunable oxygen vacancy. The key step is that TiCl₃ aqueous solution was employed as starting materials to make oxygen vacancy uniformly dispersed in the whole TiO₂ nanocrystals. Zn powder was added into the reaction to avoid the oxidation of Ti³⁺, and tune oxygen vacancy concentration and crystalline phase. When the addition amount of Zn powder increases,

the color of reduced TiO₂ nanocrystals gradually turns into dark blue and rutile phase. That means reduced TiO₂ in rutile phase is more stable. The blue TiO_{2-x} rutile nanorods can be stored at room temperature over a year without activity-loss. The photocatalytic performance of TiO_{2-x} reaches maximum, when the all TiO₂ nanocrystals just turned into rutile phase.

In typical, 1 mL of TiCl₃ (15-20%) aqueous solution was added into 30ml isopropanol, and then Zn powder (0.5-2.5 mmol) was added into above solution. After stirring about 30 min, the mixture solution was transferred into a dried Teflon autoclave container. Then the reaction was placed into 180°C oven for 6 hours. The obtained solid was collected and washed with 100 mL of 4 mol/L HCl aqueous solution over 12 hours to remove excess Zn powder. After that, the solid was washed with distilled water 3 times, and then dried at 70°C. EDAX results (Fig. S1) indicate that no Zn signal is observed. That reveals the Zn has been totally removed by acid washing step.

When TiCl₃ aqueous solution was added into water, the color of solution turned from blue purple into transparent within a short period, indicating that the Ti³⁺ is easily oxidized to Ti⁴⁺. Only white anatase TiO₂ nanocrystals are obtained after hydrothermal reaction (Fig. S2). Isopropanol is chosen as solvent instead of water due to Ti³⁺ can survive in the isopropanol solution. After solvothermal reaction, gray TiO₂ nanocrystals were obtained. X-ray diffraction (XRD) pattern (Fig. S3) indicate that the obtained TiO₂ is the mixture of anatase and rutile TiO₂, indicating that the most of Ti³⁺ is oxidized and forms TiO₂ in the solvothermal reaction. To avoid the oxidation of Ti³⁺, Zn powder is added into the solvothermal reaction. The as-prepared TiO₂ nanocrystals show a series color change from gray to dark blue with the addition of different amount Zn (Fig. 1C insets). The UV-Vis spectra of reduced TiO₂ nanocrystals, as shown in Fig. 1A, disclose that a broad absorption band appears in the visible region and it turns stronger with the addition amount of Zn powder. When the Zn powder amount increases to 1.5 mmol, the optical band gap of reduced TiO₂ changed to 2.93 eV (Fig. S4). Fig. 1B shows the XRD patterns of the reduced TiO₂ nanocrystals samples. The relative amount of rutile phase in the reduced TiO₂ gradually increases with increasing the amount of Zn powder. When 1.5 mmol Zn powder was added into the reaction, the only rutile TiO₂ nanocrystals were obtained. Although Huang *et al* obtained the Ti³⁺ self-doped TiO₂ through hydrothermal route with Zn powder and Ti⁴⁺, Zn²⁺ was detected at the surface of TiO₂ nanocrystals.^{3f} In our case, no Zn signal is observed in the EDAX (Fig. S1) and X-ray photoelectron spectroscopy XPS full scan spectra (Fig. S5). High resolution XPS of Ti 2p, as shown in Fig. 1C, reveals that the peaks at 458.3 and 464.1 eV, attributed to Ti 2p 3/2 and Ti 2p 1/2, shift to low binding energy 457.8 and 463.5 eV, respectively. This shift indicates that the Ti³⁺ doped TiO₂ forms and the oxygen vacancy concentration increases in the TiO₂ nanocrystals with the increase of Zn powder amount. Electron paramagnetic resonance (EPR) spectroscopy was employed to determine the presence of Ti³⁺. A strong EPR signal is observed at g=1.96 (Fig. 1D), which could be assigned to Ti³⁺,¹⁵ thus confirming the existence of the Ti³⁺ in the nanorods. No EPR signal at g=2.02 implies that all of the Ti³⁺ located in the bulk, which is crucial for the stability of our reduced TiO₂ nanorods.^{3d}

Fig. 2 shows transmission electron microscopy (TEM) images of the reduced TiO₂ nanocrystals prepared by the solvothermal reaction with different amount of Zn powder. When the Zn powder amount is lower than 0.5 mmol, the TiO₂ nanocrystals are mainly in anatase phase and in truncated octahedron (Fig. 2A). High resolution TEM image (inset) also shows clear 0.35 nm lattice fringes, corresponding to (101) lattice plane of anatase TiO₂. When Zn powder amount increase to 1.0 mmol, there are two TiO₂ morphologies observed,

truncated octahedron anatase TiO₂ and rutile TiO₂ nanorods with exposed of (110) facet. Further Zn powder amount increase to 1.5 mmol, only the rutile TiO₂ nanorods with 50 nm length and ~ 5nm diameter were obtained. High-resolution TEM image disclose 0.32 nm lattice fringes, corresponding to (110) lattice plane of rutile TiO₂. Zn powder amount further increases, the TiO₂ morphology (Fig. 2D) has no obvious change. These TEM results indicate that all TiO₂ nanocrystals possess well-defined facet, for example, TiO₂ rutile nanorods exposed (110) facet. Small aggregation composed with a few TiO₂ nanorods can be observed in the SEM images (Fig. S6). The N₂ absorption was employed to evaluate the surface area of obtained TiO₂ nanocrystals. Fig. S7 shows the N₂ absorption curves, which exhibit typical type IV curves. The BET surface area of TiO₂ nanocrystals gradually decreases from 90 m²/g to 55m²/g for from anatase TiO₂ truncated octahedron to rutile nanorods, respectively.

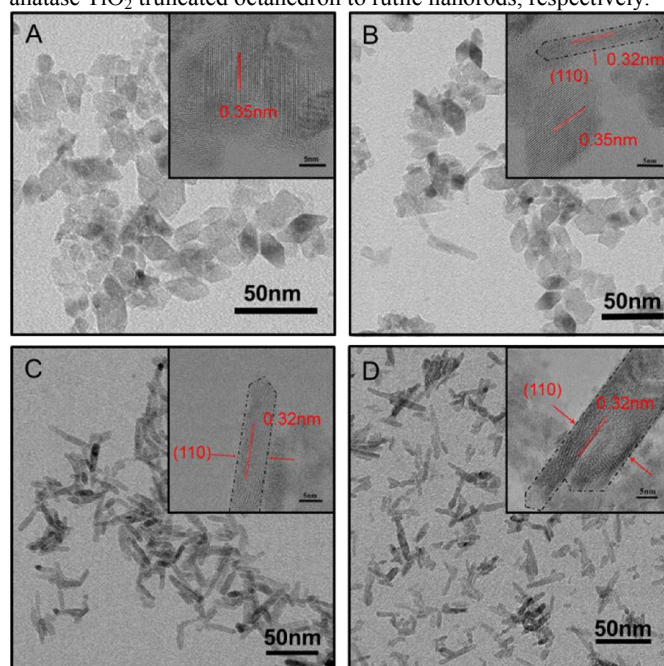


Fig. 2 TEM images of reduced TiO₂ prepared by solvothermal reaction in presence of 0.5, 1.0, 1.5 and 2.5 mmol of Zn powder. Insets are the corresponding high-resolution TEM images.

Photocatalytic water splitting H₂ production was used to evaluate the photocatalytic activity of as-obtained TiO_{2-x} nanocrystals. Fig. 3A shows typical time course of H₂ evolution under full solar spectrum (Xe lamp 300W). Normal rutile nanoparticles (~ 30 nm in diameter purchased from Aladdin Reagent. Inc.) shows very weak photocatalytic activity. Rutile TiO₂ nanorods prepared from reduced TiO₂ nanorods calcined at 450 °C for 30 min, shows ~ 0.14 mmol/h per 0.1g photocatalyst. For the reduced TiO₂, the H₂ evolution amount at same time period increases with the increase of rutile ratio in mixture reduced TiO₂ nanocrystals. H₂ production amount reach maximum ~0.6 mmol/hour for 0.1 g reduced TiO₂ when reduced TiO₂ completely transfer into rutile phase. After that, the H₂ evolution amount decreases, indicating that the photocatalytic performance decrease in the case of too high oxygen vacancy concentration, which produced by the over-reduction of excess amount Zn powder. Under visible light ($\lambda > 420$ nm, Xe lamp with a 420 nm cut-off filter), the H₂ evolution curve is exhibited in Fig. 3B. The reduced TiO₂ rutile nanorods show a stable H₂ release rate of ~ 8 μ mol/hour per 0.1g photocatalyst. The normal Rutile TiO₂ nanoparticles and TiO₂ nanorods with defined facets show no H₂ production under visible light ($\lambda > 420$ nm). The probably

mechanism is that the oxygen vacancy narrow the band gap of TiO₂ and promote the charge separation of photo generated charge carriers (Fig. S9). The photocatalytic activity is still kept without noticeable decrease after five times recycles (Fig.3D), demonstrating the excellent stability of the reduced TiO₂.

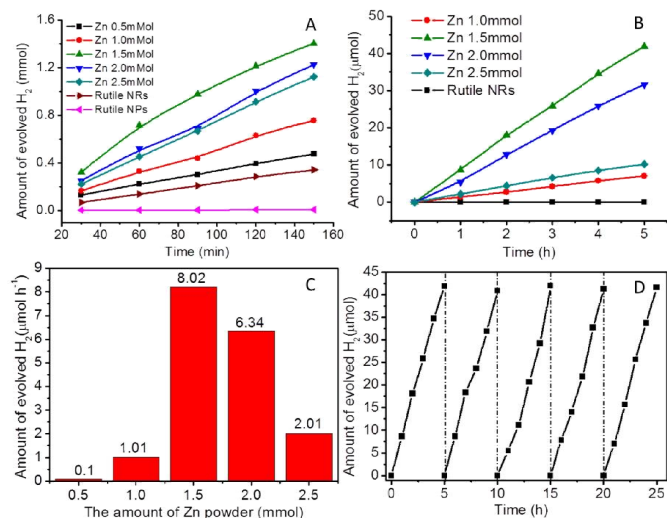


Fig. 3 Time courses of H₂ production from reduced TiO₂ loaded with 0.5% Pt in 20% methanol/ water under Xeon lamp (300W) without (A) and with (B) UV-420 cut-off filter illumination. (C) H₂ production rate for reduced TiO₂ prepared from different amount of Zn powder under visible light ($\lambda > 420\text{nm}$). (D) Cycling tests of photocatalytic activity of reduced TiO₂ prepared from 1.5 mmol Zn powder under visible light ($\lambda > 420\text{nm}$). Rutile NPs is TiO₂ nanoparticles with $\sim 30\text{ nm}$ in diameter. Rutile NRs was prepared reduced TiO₂ calcined at 450 °C for 30min.

In conclusion, we have developed a simple one-step method to synthesize reduced TiO₂ rutile nanorods with well-defined facets. The as-prepared reduced TiO₂ exhibits high stability in air and water with light irradiation. The reduced degree (oxygen vacancy concentration) can be tuned by the addition amount of Zn powder. Experimental results show good conversion efficiency in both full solar spectrum and visible light ($\lambda > 420\text{nm}$), which support that it is the introduced oxygen vacancy that accounts for the extension of the photocatalytic activity from the UV to the visible light region. Excess amount of oxygen vacancy will result in a decrease of photocatalytic performance. The present study demonstrates a simple and economical method for narrowing the band gap and for the development of a highly active photocatalyst under visible light.

Financial support from the National Natural Science Foundation of China (No. 21201159, 61176016, and 21104075), the Science and Technology Department of Jilin Province (No. 20121801), "Hundred Talent Program" CAS and open research fund of Key Laboratory of Functional Inorganic Material Chemistry (Heilongjiang University).

Notes and references

^a State Key Laboratory of Luminescence and Applications, Changchun Institute of Optics, Fine Mechanics and Physics, Chinese Academy of Sciences (CAS), Changchun, Jilin 130033, China.

^b University of Chinese Academy of Sciences, Beijing 100000, China

^c Dalian National Laboratories for Clean Energy, Dalian Institute of Chemical Physics, CAS, Dalian, Liaoning 116023, China.

^d State Key Laboratory of Inorganic Synthesis and Preparation, Jilin University, Changchun, Jilin 130012, China

Electronic Supplementary Information (ESI) available: Detailed experiments and characterization, XRD, SEM, N₂ adsorption. See DOI: 10.1039/c000000x/

- a) M. Graetzel, R. A. J. Janssen, D. B. Mitzi and E. H. Sargent, *Nature*, 2012, **488**, 304-312. b) Hagfeldt, G. Boschloo, L. Sun, L. Kloo and H. Pettersson, *Chem. Rev.*, 2010, **110**, 6595-6663. c) X. Chen, S. Shen, L. Guo and S. S. Mao, *Chem. Rev.*, 2010, **110**, 6503-6570. d) A. L. Linsebigler, G. Lu and J. T. Yates, *Chem. Rev.*, 1995, **95**, 735-758. e) H. Chen, C. E. Nanayakkara and V. H. Grassian, *Chem. Rev.*, 2012, **112**, 5919-5948. f) J. Su, X. Zou, G. D. Li, Y. M. Jiang, Y. Cao, J. Zhao, J. S. Chen, *Chem. Commun.* 2013, **49**, 8217-8219.
- a) M. Anpo, *Pure Appl. Chem.*, 2000, **72**, 1787-1792. b) A. Fuente, M. D. Hernandez-Alonso, A. J. Maira, A. Martinez-Arias, M. Fernandez-Garcia, J. C. Conesa and J. Soria, *Chem. Commun.*, 2001, 2718-2719. c) B. Liu, H. M. Chen, C. Liu, S. C. Andrews, C. Hahn and P. Yang, *J. Am. Chem. Soc.*, 2013, **135**, 9995-9998. d) J. Cao, Y. Zhang, L. Liu and J. Ye, *Chem. Commun.*, 2013, **49**, 3440-3442. e) R. Asahi, T. Morikawa, T. Ohwaki, K. Aoki and Y. Taga, *Science*, 2001, **293**, 269-271. f) F. Dong, S. Guo, H. Wang, X. Li and Z. Wu, *J. Phys. Chem. C*, 2011, **115**, 13285-13292. g) S. In, A. Orlov, R. Berg, F. Garcia, S. Pedrosa-Jimenez, M. S. Tikhov, D. S. Wright and R. M. Lambert, *J. Am. Chem. Soc.*, 2007, **129**, 13790-13791. h) G. Liu, Y. Zhao, C. Sun, F. Li, G. Q. Lu and H.-M. Cheng, *Angew. Chem. Int. Ed.*, 2008, **47**, 4516-4520. i) S. G. Kumar and L. G. Devi, *J. Phys. Chem. A*, 2011, **115**, 13211-13241.
- a) I. Justicia, P. Ordejón, G. Canto, J. L. Mozos, J. Fraxedas, G. A. Battiston, R. Gerbasi and A. Figueras, *Adv. Mater.*, 2002, **14**, 1399-1402. b) F. Zuo, L. Wang, T. Wu, Z. Zhang, D. Borchardt and P. Feng, *J. Am. Chem. Soc.*, 2010, **132**, 11856-11857. c) X. Chen, L. Liu, P. Y. Yu and S. S. Mao, *Science*, 2011, **331**, 746-750. d) F. Zuo, K. Bozhilov, R. J. Dillon, L. Wang, P. Smith, X. Zhao, C. Bardeen and P. Feng, *Angew. Chem. Int. Ed.*, 2012, **51**, 6223-6226. e) Z. Zheng, B. Huang, J. Lu, Z. Wang, X. Qin, X. Zhang, Y. Dai and M.-H. Whangbo, *Chem. Commun.*, 2012, **48**, 5733. f) Z. Zheng, B. Huang, X. Meng, J. Wang, S. Wang, Z. Lou, Z. Wang, X. Qin, X. Zhang and Y. Dai, *Chem. Commun.*, 2013, **49**, 868-870. g) J. Su, X. Zou, Y. Zou, G. D. Li, P. P. Wang, J. S. Chen, *Inorg. Chem.* 2013, **52**, 5924-5930
- D. C. Cronemeyer, *Phys. Rev.*, 1959, **113**, 1222-1226.
- J. Nowotny, T. Bak, M. K. Nowotny and L. R. Sheppard, *J. Phys. Chem. B*, 2006, **110**, 18492-18495.
- M. K. Nowotny, L. R. Sheppard, T. Bak and J. Nowotny, *J. Phys. Chem. C*, 2008, **112**, 5275-5300.
- V. N. Kuznetsov and N. Serpone, *J. Phys. Chem. C*, 2009, **113**, 15110-15123.
- V. E. Henrich and R. L. Kurtz, *Phys. Rev. B*, 1981, **23**, 6280-6287.
- H. Liu, H. T. Ma, X. Z. Li, W. Z. Li, M. Wu and X. H. Bao, *Chemosphere*, 2003, **50**, 39-46.
- Y. Li, X. Li, J. Li and J. Yin, *Mater. Lett.*, 2005, **59**, 2659-2663.
- G. Wang, H. Wang, Y. Ling, Y. Tang, X. Yang, R. C. Fitzmorris, C. Wang, J. Z. Zhang and Y. Li, *Nano Lett.*, 2011, **11**, 3026-3033.
- G. A. Kimmel and N. G. Petrik, *Phys. Rev. Lett.*, 2008, **100**, 196102.
- S. Hashimoto and A. Tanaka, *Surf. Interface Anal.*, 2002, **34**, 262-265.
- X. Liu, S. Gao, H. Xu, Z. Lou, W. Wang, B. Huang and Y. Dai, *Nanoscale*, 2013, **5**, 1870-1875.
- J. C. Conesa and J. Soria, *J. Phys. Chem.*, 1982, **86**, 1392-1395.

TOC Figure

Enhanced visible-light photocatalytic performance for water splitting H_2 evolution is obtained from reduced TiO_2 rutile nanorods with well-defined facets.

